RSC Advances

ROYAL SOCIETY OF CHEMISTRY

www.rsc.org/advances

Cite this: DOI: 10.1039/c0xx00000x

www.rsc.org/xxxxxx

ARTICLE TYPE

Role of organic solvent addition to ionic liquid electrolytes for lithium-sulphur batteries

Shizhao Xiong,[a,b] Johan Scheers,[b] Luis Aguilera,[b] Du-Hyun Lim,[b] Kai Xie,[a] Per Jacobsson[b] and Aleksandar Matic*[b]

Received (in XXX, XXX) Xth XXXXXXXXX 20XX, Accepted Xth XXXXXXXXX 20XX
DOI: 10.1039/b000000x

We investigate the role of the addition of an organic solvent to an ionic liquid electrolyte for the performance of lithium-sulphur (Li-S) batteries. We find that with a mixed electrolyte, formed by adding 10 wt% 1,3-dioxolane (DIOX) to an ionic liquid, the capacity of a Li-S cell is more than doubled, the rate capability and the cycling performance considerably improved, compared to a cell utilizing a neat ionic liquid electrolyte. The improved performance can be correlated with an enhanced ion transport, evidenced by an increased ionic conductivity and higher limiting current density, directly related to a decrease in viscosity and glass transition temperature of the mixed electrolytes. We show that this in turn is linked to a change in the local environment of the Li-ions where the organic solvent is incorporated in the coordination shell. In addition we show that the mixed electrolytes have a considerably higher thermal stability, in particular a dramatically increased flash point, and improved low temperature properties with respect to a conventional organic solvent based electrolyte currently used for Li-S batteries.

Introduction

The energy density of commercial lithium ion batteries is currently not enough for key applications in a future sustainable society, such as electric vehicles (EVs) and large scale energy storage for load levelling in the smart grid.[1,2] Out of several options for the next generation battery systems, the lithium-sulphur technology is one of the most promising candidates owing to the combination of a high theoretical energy density and potential for sustainability and competitive price, the latter related to the large abundance and low cost of sulphur.[2,3] However, before the technology can be realised in practise central issues concerning capacity fading and loss of active material, both related to the solubility of polysulfides in the electrolyte, have to be addressed. Considerable advances have been achieved in understanding the mechanisms and improving the electrochemical performance of lithium-sulphur batteries.[4-6] Recent progress has in particular been made on the cathode side through new opportunities offered by nano-structured materials[7], such as nanoporous carbon-sulphur composites,[8] graphene-sulphur composites,[9,10] and nanostructured Li_2S cathodes.[11,12] However, this has not been matched by a corresponding development of the electrolyte.

The most common electrolyte solutions are today based on organic solvents doped with lithium salts,[13-17] even though several other systems have also been considered, such as glass-ceramics[18] or polymer electrolytes.[19] Among the organic solvent based electrolytes a mixture of 1,3-dioxolane (DIOX) and 1,2-dimethoxyethane (DME) (1:1, v/v) doped with the Li-salt $LiN(CF_3SO_2)_2$ (LiTFSI) has been widely used in laboratory scale lithium-sulphur cells, due to a low viscosity and high solubility for polysulfides.[20-22] However, as for other types of Li-batteries electrolytes based fully on organic solvents present a serious safety issue related to their volatility, manifested in a low flash point and high flammability.[14,15,23,24] DIOX is in this respect particularly hazardous with a flash point around 0°C.[25]

Room temperature ionic liquids (RTILs) have in recent years been highlighted as a base for safe electrolytes in Li-batteries as well as for other electrochemical devices.[26,27] Ionic liquids are molten salts with general properties such as a very low vapour pressure and high intrinsic ionic conductivity. With the right combination of anion and cation they can also be made to have wide electrochemical window, high thermal stability and nonflammability thus mitigating the safety problems found for organic solvent based electrolytes.[26,28-30] Some RTILs based electrolytes have already been proposed for lithium-sulphur battery applications. Most common systems are based on the bis(trifluoromethanesulfonyl)imide anion (TFSI) combined with N-methyl-(n-butyl)pyrrolidinium (PYR14),[31] 1-ethyl-3-methylimidazolium (EMIM)[32] or N,N-diethyl-N-methyl-N-(2-methoxyethyl)ammonium (DEME)[33] cations and doped with LiTFSI. However, the relatively high viscosity and strong complexation of the Li-ion with the TFSI-anion results in a relatively low mobility of lithium ions in RTILs.[34] The introduction of an organic solvent to the ionic liquid offers a route to improve this situation. For Li-ion batteries it has been shown that the addition of an organic solvent, as a minority component (<40 wt%), can improve transport properties while keeping the beneficial properties of the ionic liquids regarding the low volatility and low flammability.[35] In the case of Li-sulphur

batteries the solubility of polysulfides could potentially also be improved.

In this work, we present a systematic study on the role of the addition of an organic solvent on the functionality of ionic liquid based electrolytes for lithium-sulphur batteries. We have investigated the mixtures of the ionic liquid PYR14-TFSI, which has shown very promising properties in Li-ion batteries, and the organic solvent DIOX which is among the organic solvents giving the best performance in lithium-sulphur battery studies so far. We report results on the effect on the capacity and cyclability of the battery as well as the transport properties, thermal and phase behaviours, and ionic interactions in the mixed electrolytes. We show that the capacity of the battery is more than doubled when just 10wt% of the organic solvent is added to the ionic liquid. The lithium-sulphur cell with the mixed electrolyte also shows a very good cyclability and high coulombic efficiency. This improvement can be traced back to a significantly enhanced ionic conductivity and Li-ion transport obtained from a decrease in the interaction between the Li-ions and the TFSI-anion in the electrolyte. In addition the low temperature properties of the electrolyte are improved as the addition of the organic solvent inhibits crystallization of the ionic liquid at low temperatures.

Experimental

Materials

1,3-dioxolane (DIOX, reagent grade, Sigma-Aldrich), Lithium bis(trifluoromethylsulfonyl)imide salt (LiTFSI, 99.95%, Sigma-Aldrich) and N-methyl-(n-butyl)pyrrolidinium bis(trifluoromethylsulfonyl)imide (PYR14-TFSI, 99.9%, Solvionic) were stored in a glove box under argon atmosphere and used as received. Mixed electrolytes were prepared by stirring (400 rpm) DIOX, PYR14-TFSI and LiTFSI (LiTFSI concentration, 0.4 mol kg^{-1}) for 24 hours.

Electrolyte characterization

According to the measurement protocol D6450 by Grabner,[36] the flash point – T(flash) – was determined for 1ml of sample heated in a closed cup from T(initial) to T(final). To follow the protocol exactly, T(initial) should be equal to T(flash) minus 18°C and T(final) should be high enough to detect T(flash). T(flash) is defined as the temperature where the ignition of the fumes produce an increase in pressure that surpass a predefined criterion (20 kPa) under a certain air flow, heating rate (5.5°C/min) and ignition interval (1test/°C).

The ionic conductivity was measured on a Novocontrol broadband dielectric spectrometer in the temperature range -25 - 45°C in a gold-plated cell with 100 µm glass fibre spacers. A symmetrical cell, Li/electrolyte/Li (10 mm diameter, Li-foil from Chemetall Foote Corp., separator from Celgard® 2400, 20µm) was used to investigate the Li-ion transport in the electrolytes. DC polarization experiments with the symmetrical cells were performed using a multi-channel electrochemical analyser (Ivium-n-Stat instrument, Ivium Technologies B.V.) at discrete voltage steps from open circuit voltage (OCV < 3mV).

The viscosity of the mixed electrolytes was determined by a Lovis 2000 M/ME (Anton Paar) viscosity meter in the temperature range 10°C and 50°C. Differential Scanning Calorimetry (DSC) measurements were performed using a Q1000 TA instrument under He flow. The samples were cooled to -120°C, cooling rate of 20°C/min, equilibrated at that temperature for 5 minutes, and subsequently heated to 40°C at a heating rate of 10°C/min. The thermal transitions were determined from the heating scan. The glass transition temperature was taken as the mid-point of the heat capacity step-change from the amorphous glass state to the liquid state and the melting temperature as the minimum value of the endothermic peak. Thermogravimetric analysis (209 TG F1, Netzsch) was performed in the temperature range 25 - 600°C at a heating rate of 10°C /min under flow of N_2. Raman spectra were recorded on a Bruker IFS66 Fourier Transform spectrometer with a FRA106 Raman module. The excitation source is the 1064 nm line of a Nd:YAG laser and the laser power was set to 60 mW. The spectra were recorded with a resolution of 2 cm^{-1} and were averaged of over 5000 scans.

Evaluation in coin cells

Sulphur cathodes were prepared by mixing sulphur powder (reagent grade, Sigma-Aldrich), acetylene black (Alfa) and polyvinylidene fluoride (PVDF, Mw=534,000, Sigma-Aldrich) at a weight ratio of 60:30:10 in N-methyl-2-pyrrolidinone (NMP, 99.5%, Sigma-Aldrich). The suspension was mixed in a spex ball mill at room temperature for 2.5 h at 580 rpm. The slurry was coated on an aluminium current collector and subsequently dried at 80°C under vacuum for 24h to allow complete solvent evaporation. Lithium-sulphur coin cells were assembled with the sulphur cathode (10 mm diameter), lithium disks (10 mm diameter, Chemetall Foote Corp), a separator (20µm, Celgard® 2400) and the mixed electrolytes. Galvanostatic charge and discharge experiments were performed between 1.5 V and 2.5 V using a multi-channel electrochemical analyser (Ivium-n-Stat instrument, Ivium Technologies B.V.).

Results and discussion

Fig. 1 shows the discharge-charge profiles of lithium-sulphur cells with the ionic liquid based electrolyte and the mixed electrolyte containing 10wt% DIOX. The cell with PYR14-TFSI+0.4 mol kg^{-1} LiTFSI electrolyte delivers a capacity of 256 mAh g^{-1} sulphur at a current density of 50 mA g^{-1}. With increasing discharge-charge rate the capacity of the cell decreases, a common problem for Li-S cell.[37] The capacity determined here is only 15% of the theoretical capacity, which suggests that the electrochemical reaction of the active material is not very efficient. This can be related to both the structure of the actual cathode as well as the ability of the electrolyte to allow for sufficient reaction kinetics at the electrodes. One should note that the sulphur cathode in this work is far from optimised, just prepared by ordinary ball milling of the sulphur powder and acetylene black, which to a large extent explains the lower capacity. A higher capacity of the cell would be achieved if a more advanced cathode, e.g. the nanostructured sulphur cathode as reported in ref,[7] would be used. However, as the aim of the current work is to investigate the applicability of mixed electrolytes the use of a rather simple cathode is sufficient in order to monitor relative effects of different electrolytes. Even though the capacity is not very high one can note that the cell has a high coulombic efficiency, up to 99%, showing a high

reversibility in the utilization of active material in the electrochemical reactions.

The addition of DIOX to the ionic liquid electrolyte clearly improves the performance of the cell with a more than doubled capacity, 550 mAh g^{-1} sulphur at a current density of 50 mA g^{-1}. This enhancement is even larger for higher charge-discharge rates, at the highest rate the capacity is a factor six higher when using the mixed electrolyte compared to the neat ionic liquid electrolyte. Although the absolute capacity of the cell with the mixed electrolyte is lower than previously reported,[38] it displays an attractive cycling performance as shown in Fig. 1. After 30 cycles with different rates, the cell retains a capacity close to the initial cycle, thus capacity fading is very low.

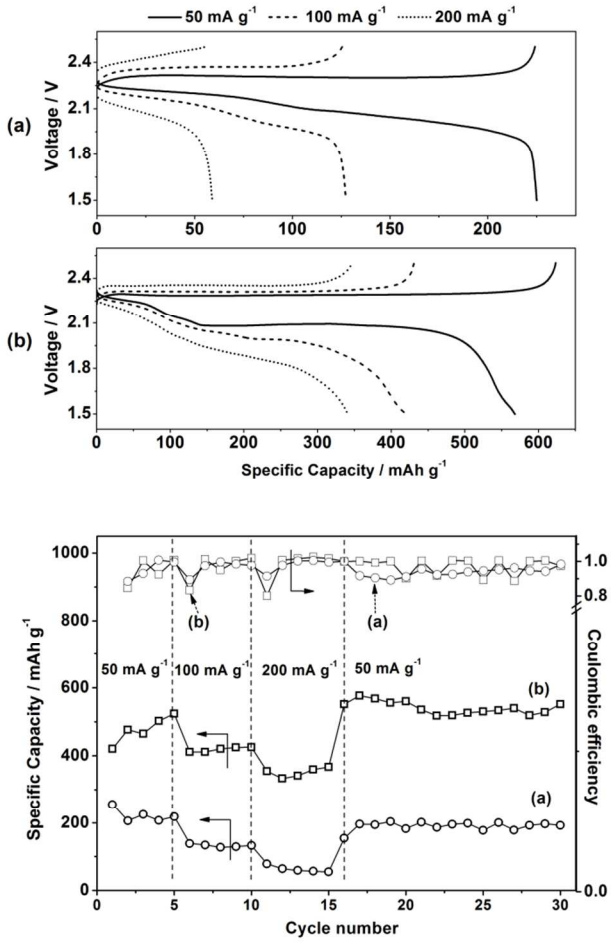

Fig. 1 Top: Discharge-charge profile of lithium-sulphur cells at different discharge rates and with (a) PYR14-TFSI+0.4 mol kg^{-1}LiTFSI electrolyte and (b) 10wt%DIOX+90wt%PYR14-TFSI+0.4 mol kg^{-1}LiTFSI electrolyte. Bottom: Specific capacity as function of cycle number and discharge rate for the lithium-sulphur cells with (a) PYR14-TFSI+0.4 mol kg^{-1}LiTFSI electrolyte and (b) 10wt%DIOX+90wt%PYR14-TFSI+0.4 mol kg^{-1}LiTFSI electrolyte.

Previous publications have suggested that the enhancement of the electrochemical performance can be attributed to the improved mobility of Li-ions and the ionic conductivity of the electrolytes.[39] Fig. 2 shows the ionic conductivity as a function of temperature for the mixed electrolytes. The ionic conductivity follows the expected behaviour of a liquid electrolyte, a decrease with decreasing temperature due to an increase in the viscosity,[39] as shown in Fig. S1, in the Supplementary information. With the addition of the organic solvent, DIOX, there is a decrease in the viscosity, see Fig. S1, and a concurrent increase in the ionic conductivity. The improvement is particularly notable at low temperatures. With the addition of 10wt% DIOX to the ionic liquid the ionic conductivity at -25°C is one order of magnitude higher than in the neat ionic liquid electrolyte and with 20wt% DIOX, the ionic conductivity at -25°C is of the order of 1 mS cm^{-1}.

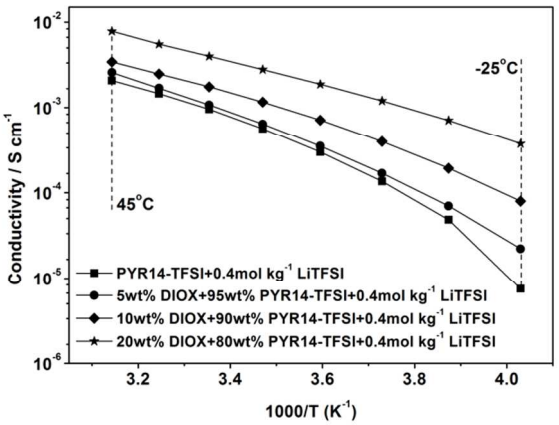

Fig. 2 Ionic conductivity as a function of temperature for the mixed electrolytes.

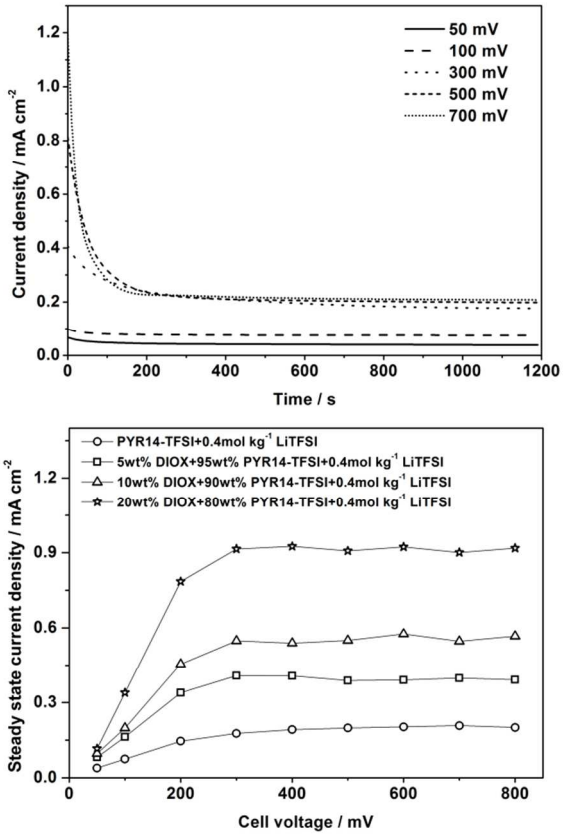

Fig. 3 Top: Chronoamperograms for a symmetrical cell with PYR14-TFSI+0.4 mol kg^{-1} LiTFSI electrolyte at various voltages. Bottom: Steady state current density obtained from a symmetrical cell with mixed electrolytes.

To obtain more direct information on the Li-ion mobility, in conductivity the contributions from all ions present are summed up, chronoamperometry in symmetric Li/electrolyte/Li cells can be used. The steady state current observed after polarization of the symmetric cell is directly related to the Li-ion transport.[34] Fig. 3 shows the results from such experiments under various polarization voltages for the ionic liquid electrolyte and the mixed electrolytes. A large initial current, that decays rather rapidly, is observed after each voltage step. This phenomenon suggests that the transference number of Li^+ in the electrolyte is, as expected, less than unity due to the contribution from other ions in the electrolyte. The decaying current is related to the formation of a concentration gradient of Li^+ in the electrolyte during lithium deposition at the cathode and striping from the anode.[34] Since the anion and the cation of the ionic liquid (PYR14 and TFSI) cannot be transferred at the lithium electrodes, the steady state current entirely corresponds to the current carried by Li^+ and is controlled by charge migration in the electrolyte and charge transfer at the lithium electrode/electrolyte interface.[40] In Fig. 3 steady state currents as a function of the applied voltage are shown for the electrolytes with different concentration of DIOX. The steady state currents increase with increasing voltage in the range from 50 mV to 300 mV and then levels off. The levelling off of the limiting current as a function of applied voltage suggests that the electrochemical reactions on electrodes are limited by Li^+ diffusion in the electrolyte. As shown in Fig. 3, the liming current increases considerably with the increasing DIOX concentration in the electrolytes which is direct evidence of improved Li^+ transport in the mixed electrolytes.

High thermal stability is another key property of ionic liquid based electrolytes when it comes to battery applications. As seen in Fig. 4 and table I the neat ionic liquid electrolyte is very stable. It shows no weight loss up to more than 300°C in the TGA experiment and no flash point could be detected up to 200°C (maximum of the equipment). In contrast, the organic solvent based electrolyte (DIOX+0.4 mol kg^{-1} LiTFSI) is very volatile and the flash point is very low, around 0°C[25]. In the case of the mixed electrolytes we clearly see that the presence of the ionic liquid improves the thermal stability both in the case of weight loss in the TGA experiment and in the flash point. With decreasing amount of DIOX the flash point rapidly increases and is above 50°C for 5wt% DIOX in the ionic liquid electrolyte. Thus, the thermal characteristics lead to a considerable improvement in safety with the mixed electrolytes.

An additional positive feature of the mixed electrolytes is the very high low temperature conductivity. This can be traced back to the phase behaviour of the electrolytes as shown in the bottom graph of Fig. 4 and in Table II where the phase transition temperatures are summarized. The neat ionic liquid electrolyte displays a glass transition at -79°C and a melting point at -19°C, in agreement with previous results in literature.[41] The organic solvent based electrolyte (DIOX+0.4 mol kg^{-1} LiTFSI) exhibits a glass transition at -97°C and a melting process at -55°C. Thus both the ionic liquid electrolyte and the organic solvent based electrolytes are prone to crystallize at low temperature limiting the temperature window of application. In contrast all the mixed electrolytes only show a glass transition, and no melting transition, showing that crystallization is effectively supressed in the mixtures. Thus the addition of the organic solvent enhances the effective liquid range of the ionic liquid electrolyte improving the applicability of a Li-S battery at low temperatures. With increasing amount of DIOX the glass transition for the mixtures decreases, resulting in a lower overall viscosity and thus a higher conductivity of electrolytes contributing to the improvement in the transport performance.[42, 43]

Table I Flash points (T(flash)) of the mixed electrolytes *x* wt% PYR14-TFSI+ *y* wt% DIOX + 0.4 mol kg^{-1} LiTFSI

x	*y*	T(initial) / °C	T(flash) / °C
95	5	30	51
90	10	5	33
80	20	10	19
0	100	Closed Cup: -6°C. Open Cup: 2°C. (Material Safety Data Sheet, http://www.msds.com/)	
100	0	no T(flash) detected > 200 °C	

Table II Glass transition temperatures, T_g, and melting points, T_m, of *x* wt% PYR14-TFSI+ *y* wt% DIOX + 0.4 mol kg^{-1} LiTFSI

x	*y*	T_g (°C)	T_m (°C)
0	100	-97	-55
100	0	-79	-19
95	5	-85	—
90	10	-97	—
80	20	-105	—

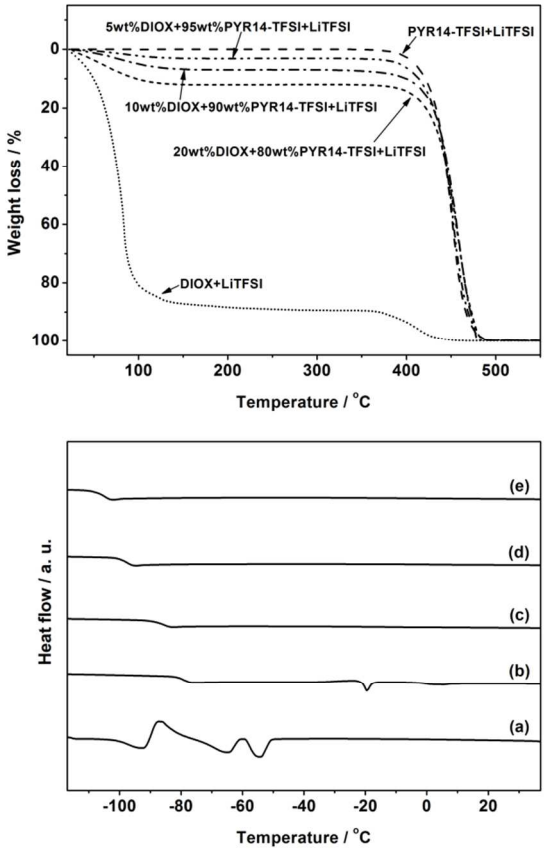

Fig. 4 Top: Weight loss as a function of temperature for the mixed electrolytes as indicated in the figure. Bottom: DSC traces for (a) DIOX+0.4 mol kg^{-1} LiTFSI, (b) PYR-14TFSI+0.4 mol kg^{-1} LiTFSI, (c) 5wt%DIOX+95wt%PYR14-TFSI+0.4 mol kg^{-1} LiTFSI, (d)

10wt%DIOX+90wt%PYR14-TFSI+0.4 mol kg^{-1} LiTFSI and (e) 20wt%DIOX+80wt%PYR14-TFSI+0.4 mol kg^{-1} LiTFSI.

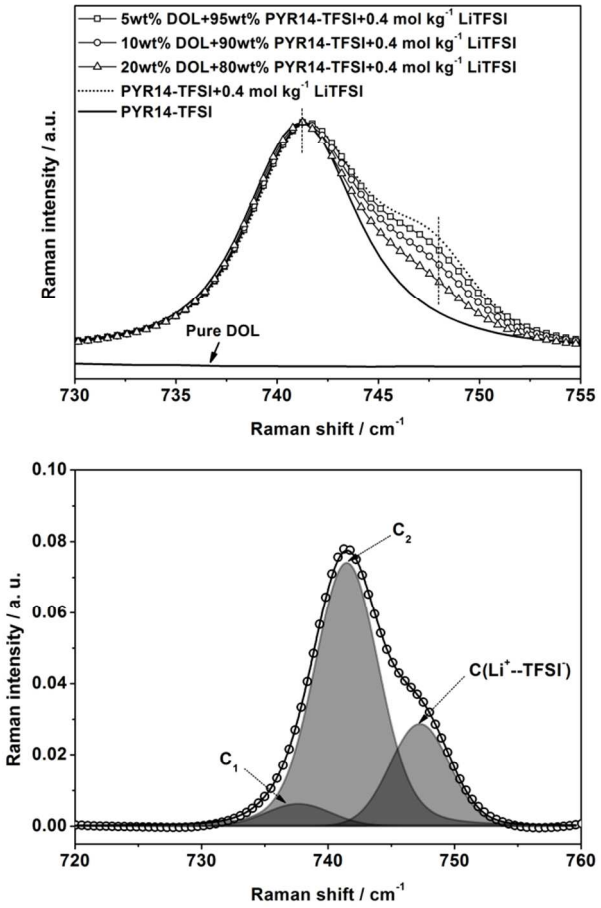

Fig. 5 Top: Raman spectra of the mixture electrolytes in the region around 740 cm^{-1}. Those spectra have been normalized by height. Bottom: Best fit to the Raman spectrum in the region around 740 cm^{-1}

On a microscopic scale the Li-ion transport properties of the mixed electrolytes are directly related to the local environment around the Li-ions. It has previously been shown that in an ionic liquid electrolyte based on the LiTFSI salt the Li-ions are coordinated to two TFSI anions in a bidental configuration at this LiTFSI concentration.[43-45] This configuration is rather stable and thus the diffusion of the Li-ion actually takes place mainly through the diffusion of the $Li[TFSI]_2^-$ triplet. Raman spectra in the region of 730-755 cm^{-1} for the mixed electrolytes are shown in Fig. 5. The intense Raman line of TFSI anion at 739-742 cm^{-1}, which corresponds to the expansion and contraction of the entire anion, will be shifted to 746-750 cm^{-1} when complexes of the type $Li[TFSI]_2^-$ are formed.[42,44,46] The new band corresponding to the interaction between Li-ion and TFSI anions is clearly observed in Fig. 5 after the addition of the lithium salt to the ionic liquid (PYR14-TFSI). With the addition of the organic solvent (DIOX) there is a noticeable decrease of the band corresponding to TFSI interacting with Li^+ (the spectral component around 748 cm^{-1}). This suggests that the interaction between Li-ions and TFSI anions is changed by the presence of DIOX. For a more quantitative analysis we have fitted the spectra with three components, as shown in Fig. 5. The two lower lying bands (C1 and band C2) correspond to the two conformations of uncoordinated TFSI anions,[42,47] whereas the third band is related to Li-ions coordinated to TFSI-anions. The population of TFSI anions interacting with Li-ions can be expressed as the fraction C,

$$C = (\text{Area III}) / (\text{Total area}) \quad (1)$$

and is summarized in Table III for the mixed electrolytes. Our results clearly show that the fraction of TFSI interacting with Li-ions decreases with the increasing amount of organic solvent in the mixed electrolytes. Most likely this is a result of the incorporation of the organic solvent (DIOX) in the coordination shell of the Li-ions. This mixed environment leads to a weaker interaction between Li and TFSI with more dynamic clusters as a result and a higher mobility of the Li-ions in accordance with the data from chronoamperometry and the improved battery performance.

Table III Relative fraction of TFSI-anions coordinated to Li-ions, C, in the mixture electrolytes (*x* wt% PYR14-TFSI+ *y* wt% DIOX + 0.4 mol kg^{-1} LiTFSI).

x	*y*	C
100	0	0.33
5	95	0.29
10	90	0.26
20	80	0.23

Conclusions

From the experiments reported above we find a clear connection between the overall performance of a Li-S battery and the basic material properties when using an ionic liquid/organic solvent mixed electrolyte. The more than doubled capacity and the good cycle life of a LiS-battery where the ionic liquid based electrolyte has 10wt% DIOX added can be traced back to a more efficient ion transport, as observed in the ionic conductivity and from chronoamperometry. The improved transport properties are related to a decreased viscosity, related to a lowering of the glass transition temperature, and to a change in the local coordination of the Li-ions, as determined by Raman spectroscopy. We propose that the improved Li-ion transport thus is a result of the incorporation of DIOX in the coordination shell around the Li-ions resulting in weaker and more dynamic clusters. In addition to improving the capacity we also show that the mixed electrolytes are advantageous from the respect of large liquid range since the tendency of crystallization at low temperatures is efficiently supressed. Furthermore, the ionic liquid based mixed electrolytes are thermally much more stable than the standard electrolytes, based on for instance DIOX, as shown by a rapid increase of the flash point with increasing ionic liquid content.

Our work on a model mixture of an ionic liquid with an organic solvent in an electrolyte presents a viable way for the improvement of Li-S battery performance with respect to safety, capacity, rate capability and cycling performance. One can also envisage that by tuning the composition with respect to type of ionic liquid, organic solvent, and the concentration one can for instance also control polysulfide solubility another important aspect for Li-S batteries.

Acknowledgements

The support provided by China Scholarship Council (CSC) during a visit of Shizhao Xiong to Chalmers University of Etchnology is acknowledged. We are grateful to the support of the Areas of Advance Energy and Materials Science at Chalmers University of Technology.

Notes and references

[a] *Department of Material Science and Engineering, College of Aerospace Science and Engineering, National University of Defense Technology, Changsha, Hunan, 410073, PR China*
[b] *Department of Applied Physics, Chalmers University of Technology, 412 96 Göteborg, Sweden. Fax: +46(0)31-7722090; Tel: +46(0)31-7725176; E-mail: matic@chalmers.se*

1 P. Bruce, B. Scrosati and J.-M. Tarascon, *Angew. Chem. Int. Ed.*, 2008, **47**, 2930-2946.
2 N. S. Choi, Z. Chen, S. A. Freunberger, X. Ji, Y. K. Sun, K. Amine, G. Yushin, L. F. Nazar, J. Cho and P. G. Bruce, *Angew. Chem. Int. Ed.*, 2012, **51**, 9994-10024.
3 P. G. Bruce, S. A. Freunberger, L. J. Hardwick and J. M. Tarascon, *Nat. Mater.*, 2012, **11**, 19-29.
4 S. Evers and L. Nazar, Accounts Chem. Res., 2013, **46**, 1125-1134.
5 A. Manthiram, Y. Fu and Y. Su, Accounts Chem. Res., 2013, **46**, 1135-1143.
6 S. Xiong, K. Xie, Y. Diao and X. Hong, *Electrochim. Acta*, 2012, **83**, 78-86.
7 Y. Yang, G. Zheng and Y. Cui, *Chem. Soc. Rev.*, 2013, **42**, 3018-3032.
8 X. Ji, K. T. Lee and L. F. Nazar, *Nat. Mater.*, 2009, **2460**, 500-506.
9 H. Wang, Y. Yang, Y. Liang, J. T. Robinson, Y. Li, A. Jackson, Y. Cui and H. Dai, *Nano Lett.*, 2011, **11**, 2644-2647.
10 L. Ji, M. Rao, H. Zheng, L. Zhang, Y. Li, W. Duan, J. Guo, E. J. Cairns and Y. Zhang, *J. Am. Chem.Soc.*, 2011, **133**, 18522-18525.
11 Y. Yang, G. Zheng, S. Misra, J. Nelson, M. F. Toney and Y. Cui, *J. Am. Chem.Soc.*, 2012, **134**, 15387-15394.
12 K. Cai, M. K. Song, E. J. Cairns and Y. Zhang, *Nano Lett.*, 2012, **12**, 6474-6479.
13 L. Suo, Y.-S. Hu, H. Li, M. Armand and L. Chen, *Nat. Commun.*, 2013, **4**, 1481-1490.
14 C. Barchasz, J.-C. Leprêtre, S. Patoux and F. Alloin, *Electrochim. Acta*, 2013, **89**, 737-743.
15 C. Barchasz, J. C. Lepretre, S. Patoux and F. Alloin, *J. Electrochem. Soc.*, 2013, **160**, A430-A436.
16 H. S. Ryu, H. J. Ahn, K. W. Kim, J. H. Ahn, K. K. Cho and T. H. Nam, *Electrochim. Acta*, 2006, **52**, 1563-1566.
17 D. R. Chang, S. H. Lee, S. W. Kim and H. T. Kim, *J. Power Sources*, 2002, **112**, 452-460.
18 A. Hayashi, R. Ohtsubo, T. Ohtomo, F. Mizuno and M. Tatsumisago, *J. Power Sources*, 2008, **183**, 422-426.
19 J. Kazem, G. Mahmoudreza and P. Chen, *J. Mater. Chem. A*, 2013, **1**, 2769-2772
20 Z. W. Seh, W. Li, J. J. Cha, G. Zheng, Y. Yang, M. T. McDowell, P.-C. Hsu and Y. Cui, *Nat. Commun.*, 2013, **4**, 1331-1336.
21 T. Lin, Y. Tang, Y. Wang, H. Bi, Z. Liu, F. Huang, X. Xie and M. Jiang, *Energy Environ. Sci.*, 2013, **6**, 1283-1290.
22 M.-K. Song, E. Cairns and Y. Zhang, *Nanoscale*, 2013, **5**, 2186-2204.
23 E. Peled, Y. Sternberg, A. Gorenshtein and Y. Lavi, *J. Electrochem. Soc.*, 1989, **136**, 1621-1625.
24 H. Yamin, A. Gorenshtein, J. Penciner, Y. Sternberg and E. Peled, *J. Electrochem. Soc.*, 1988, **135**, 1045-1048.
25 http://www.msds.com, Material Safety Data Sheet.
26 M. Armand, F. Endres, D. MacFarlane, H. Ohno and B. Scrosati, *Nat. Mater.*, 2009, **8**, 621-629.
27 A. Matic and B. Scrosati, *MRS Bulletin*, 2013, **38**, 533-537.
28 M. J. Earle, J. M. Esperanca, M. A. Gilea, J. N. Lopes, L. P. Rebelo, J. W. Magee, K. R. Seddon and J. A. Widegren, *Nature*, 2006, **439**, 831-834.
29 Y. Lu, S. K. Das, S. S. Moganty and L. A. Archer, *Adv. Mater.*, 2012, **24**, 4430-4435.
30 H. Niedermeyer, J. P. Hallett, I. J. Villar-Garcia, P. A. Hunt and T. Welton, *Chem. Soc. Rev.*, 2012, **41**, 7780-7802.
31 S. Xiong, K. Xie, E. Blomberg, P. Jacobsson and A. Matic, *J. Power Sources*, 2014, **252**, 150-155.
32 J. Wang, S. Y. Chew, Z. W. Zhao, S. Ashraf, D. Wexler, J. Chen, S. H. Ng, S. L. Chou and H. K. Liu, *Carbon*, 2008, **46**, 229-235.
33 J.-W. Park, K. Yamauchi, E. Takashima, N. Tachikawa, K. Ueno, K. Dokko and M. Watanabe, *J. Phys. Chem. C*, 2013, **117**, 4431-4440.
34 J.-W. Park, K. Yoshida, N. Tachikawa, K. Dokko and M. Watanabe, *J. Power Sources*, 2011, **196**, 2264-2268.
35 L. Lombardo, S. Brutti, M. A. Navarra, S. Panero and P. Reale, *J. Power Sources*, 2013, **227**, 8-14.
36 A. Hofmann, L. Merklein, M. Schulz and T. Hanemann, *Electrochim. Acta*, 2014, **116**, 388-395.
37 A. Manthiram, Y. Fu, S.-H. Chung, C. Zu and Y. Su, *Chem. Rev.*, 2014, DOI: 10.1021/cr500062v.
38 H. S. Ryu, J. W. Park, J. Park, J.-P. Ahn, K.-W. Kim, J.-H. Ahn, T.-H. Nam, G. Wang and H.-J. Ahn, *J. Mater. Chem. A*, 2013, **1**, 1573-1578.
39 J. H. Shin and E. J. Cairns, *J. Electrochem. Soc.*, 2008, **155**, A368-A373 ・.
40 K. Yoshida, M. Tsuchiya, N. Tachikawa, K. Dokko and M. Watanabe, *J. Electrochem. Soc.*, 2012, **159**, A1005-A1012.
41 A. Martinelli, A. Matic, P. Jacobsson, L. Börjesson, A. Fernicola and B. Scrosati, *J. Phys. Chem. B*, 2009, **113**, 11247-11251.
42 J. Pitawala, J.-K. Kim, P. Jacobsson, V. Koch, F. Croce and A. Matic, *Faraday Discuss.*, 2012, **154**, 71-80.
43 J. Pitawala, A. Matic, A. Martinelli, P. Jacobsson, V. Koch and F. Croce, *J. Phys. Chem. B*, 2009, **113**, 10607-10610.
44 J.-C. Lassègues, J. Grondin and D. Talaga, *Phys. Chem. Chem. Phys.*, 2006, **8**, 5629-5632.
45 J. Pitawala, A. Martinelli, P. Johansson, P. Jacobsson and A. Matic, *J Non-Cryst Solids*, 2014, DOI: 10.1016/j.jnoncrysol.2014.08.043.
46 A. Martinelli, A. Matic, P. Johansson, P. Jacobsson, L. Börjesson, A. Fernicola, S. Panero, B. Scrosati and H. Ohno, *J. RamanSpectrosc.*, 2011, **42**, 522–528.
47 J.-C. Lassegues, J. Grondin, C. Aupetit and P. Johansson, *J. Phys. Chem. B*, 2009, **113**, 305–314.

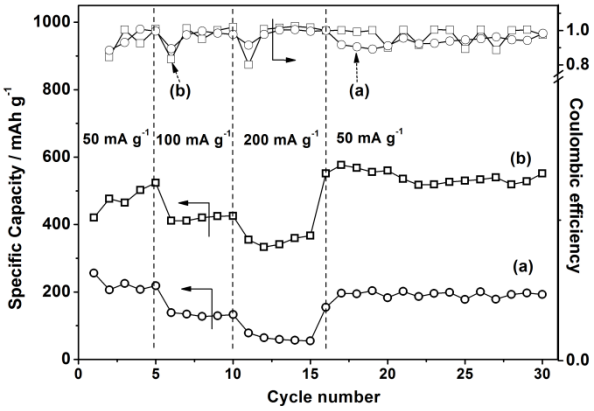

A mixed organic solvent/ionic liquid electrolyte combined the beneficial properties of both worlds, high capacity and high safety, through the local arrangement around the Li-ion.